Journal of Applied Polymer Science

Electrical Properties and the Role of Inhomogeneities at the Polyvinyl Alcohol/n-InP Schottky Barrier Interface

M. Siva Pratap Reddy,[1] Hee-Sung Kang,[2] Jung-Hee Lee,[2] V. Rajagopal Reddy,[3] Ja-Soon Jang[1]

[1]Department of Electrical Engineering, LED-IT Fusion Technology Research Center (LIFTRC), Yeungnam University, Gyeongsan-Si 712-749, South Korea

[2]School of Electrical Engineering and Computer Science, Kyungpook National University, Daegu 702-701, South Korea

[3]Department of Physics, Sri Venkateswara University, Tirupati 517-502, India

Correspondence to: J.-H. Lee (E-mail: jlee@ee.knu.ac.kr or jsjang@ynu.ac.kr)

ABSTRACT: In this work, we have investigated the electrical properties of Au/n-InP contacts with a thin layer of polyvinyl alcohol (PVA) as an interlayer. The current–voltage (I–V) and capacitance–voltage (C–V) measurements are carried out in the temperature range of 175–425 K. The Au/PVA/n-InP Schottky structure show nonideal behaviors and indicates the presence of a nonuniform distribution of interface states. The temperature dependent interface states densities (N_{SS}), ideality factor $n(V,T)$ and barrier height $\varphi_b(V,T)$ are obtained. An abnormal decrease in zero-bias barrier height (BH) and increase in the ideality factor (n) with decreasing temperature have been explained on the basis of the thermionic emission theory with Gaussian distribution (GD) of the BHs due to the BH inhomogeneities. The experimental I–V characteristics of Au/PVA/n-InP Schottky diode has revealed the existence of a double GD with mean BH values of ($\bar{\varphi}_{bo}$) of 1.246 and 0.899 eV and standard deviation (σ_o) of 0.176 and 0.137 V, respectively. Consequently, the modified conventional activation energy $\ln(I_o/T^2)-(q^2\sigma_o^2/2k_B^2T^2)$ versus $10^3/T$ plot gives $\bar{\varphi}_{bo}$ and Richardson constants (A_R^*) and the values are 1.17 and 0.71 eV and 9.9 and 6.9 A/cm^2 K^2, respectively, without using the temperature coefficient of the BH. The effective Richardson constant value of 9.9 A/cm^2 K^2 is very close to the theoretical value of 9.4 A/cm^2 K^2 for n-InP. The discrepancy between Schottky barrier heights estimated from I–V and C–V measurements is also discussed. © 2013 Wiley Periodicals, Inc. J. Appl. Polym. Sci. **2014**, *131*, 39773.

KEYWORDS: conducting polymers; sensors and actuators; surfaces and interfaces

Received 6 June 2013; accepted 18 July 2013

DOI: 10.1002/app.39773

INTRODUCTION

Schottky barrier diodes (SBD) are important in the field of electronic and optoelectronic devices. SBDs are not intimate metal/semiconductor (MS) contacts; rather, they have a metal/interfacial layer/semiconductor structure unless specially fabricated.[1] There is always native thin insulating layer (oxide) on the surface of the semiconductor in most practical MS contacts.[2] This layer converts the MS structures into metal-insulator-semiconductor structures. Many researchers have extensively investigated interfacial parameters such as the interface states and interfacial layer, because the electrical characteristics of SBDs are controlled mainly by its interfacial layer.[1–4] This interfacial layer modifies some electrical parameters of the devices like rectification performance in which the values of barrier height and ideality factors are greater than conventional MS structures. This performance and reliability has been attributed to the space charge region of the semiconductor, which is influenced by the interfacial layer in MS structures.

Developing organic/inorganic heterojunction is a promising technology due to several advantages of organic materials such as flexibility, light weight, low cost, easy manufacturing and versatile applicability. The electrical properties of the MS can be usefully modified by organic layer sandwich between the metal and semiconductor. Such type of heterojunction fabrication and the extraction of the diode parameters is an attractive research field for photovoltaic devices.[3] The organic/inorganic structures can be sensitive probe useful in establishing process for minimizing interface states, surface charges, dislocations and contaminations that may ultimately increase the quality of devices fabricated using the semiconductor. Thus, a large number of Schottky devices have been prepared and characterized using organic with metals and semiconductors.[5–10] The ultimate advantages of organic materials is their ability to be produced in large quantities by simple procedures such as spin coating, electrospinning method, high electrical conductivity and good environmental stability under ambient conditions compared to

inorganic materials. Another advantage of organic material is, when comparing to inorganic semiconductors, they do not need surfaces with regularity at the atomic level.

Many researchers have studied by using polymer as an interfacial layer at MS junction such as poly (vinylalcohol), polyaniline, poly (alkylthiophene) polypyrrole, polyophen and poly (3-hexylthiophen). Among them, polyvinyl alcohol (PVA) has unique chemical and physical property as well as its industrial applications.[11–15] In this work, PVA is selected as an interfacial layer because it has many advantages: a good surface alignment effect and photosensitivity, processing with a nonharmful solvent, low-cost material and processing, compatibility with flexible substrates, and good resistance to damage by the solvents involved in the lift-off process. Further, PVA is an interesting synthetic organic material because it is water-soluble and biocompatible, which is mainly due to hydrogen bonds between hydroxyl groups on the chain and water molecules or biomolecules. The hydrogen bonding between hydroxyl groups plays a very important role in the properties of PVA, such as its wide crystallinity and high crystal modulus. The presence of crystalline and amorphous regions in semicrystalline PVA is result from the crystal-amorphous interfacial effect. Especially, PVA has a very high dielectric strength (>1000 kV/mm) and good charge storage capacity. As a result, this can be used as passivation layer to enhance the performance of the dielectric properties of the organic thin film transistor.

In most of the previous studies,[16,17] the Schottky barrier height (SBH) was determined at room temperature by measuring the current–voltage (I–V) and capacitance–voltage (C–V) measurements of the organic Schottky devices. Analyzing the I–V and C–V characteristics of MS and MIS structures only at room temperature cannot provide us with detailed information regarding their current conduction mechanisms or the nature of barrier formation at the MS interface. However, the temperature dependence of the I–V characteristics could allow us to gain insight into different aspects of characteristics such as nature of interfacial insulator layer and carrier conduction mechanism of these devices. With this aim in mind, the electrical characteristics of the Au/PVA/n-InP Schottky structure have been studied in the temperature range of 175–425 K.

Polymer-based schemes for the fabrication of Schottky contacts on semiconductor have been extensively investigated.[18–23] For example, Gullu et al.[18] evaluated electrical characteristics of the DNA-based device in a wide temperature range. They reported that the barrier height (BH) and ideality factor (n) ranged from 0.40 eV and 2.96 at 80 K to 0.98 and 1.26 at 300 K. Soylu et al.[19] investigated temperature dependence of I–V characteristics of the Au/pyronine-B/moderately doped n-InP SBD in the temperature range 160–400 K. They achieved modification of the interfacial potential barrier using the thin interlayer of the pyronine-B. Dokme et al.[20] studied electrical and dielectric properties of Au/PVA (Ni, Zn-doped)/n-Si Schottky diodes in the temperature range 80–400 K. They showed that dielectric constant (ε'), dielectric loss (ε''), dielectric loss tangent ($\tan\delta$) are strongly temperature-dependent. Tunc et al.[21] investigated the I–V characteristics of Au/PVA/n-Si (111) SBDs in a wide temperature range. They showed that the BH (φ_{bo}) increases and ideality factor (n) decreases with an increase in temperature. Recently, Demirezen et al.[22] investigated the electrical properties of a fabricated Au/PVA (Bi-doped)/n-Si photodiode in dark and under 250 W light illumination intensity at room temperature. They reported that the high value of ideality factor and R_S are attributed to the particular distribution of interface state density (N_{SS}) at metal/PVA interface, surface and fabrication process, barrier inhomogeneity of interfacial polymer layer and the form of barrier height at MS interface. Very recently, Ozavci et al.[23] study the detailed information on the conduction mechanism of the Au/n-GaAs SBDs. They have explained the temperature dependence of forward I–V characteristics in terms of the TE mechanism with a double GD of BHs for low bias region (LBR) and moderate bias region (MBR).

In this work, we fabricate Au/n-type InP Schottky junction with a PVA interlayer and studied its electrical properties in the temperature range of 175–425 K. The SBH (φ_{bo}) and ideality factor (n) of Au/PVA/n-InP Schottky diodes are estimated at different temperatures. The possible current conduction mechanism of the Schottky contacts modified using PVA interlayer is also examined. Further, the temperature dependent of the energy distribution of interface state density (N_{SS}) profile is obtained on the basis of the variation of ideality factor with forward bias and temperature. Temperature-dependent barrier characteristics of the Au/PVA/n-InP Schottky diodes are also interpreted by using a double Gaussian distribution (GD) of the barrier heights.

EXPERIMENTAL

The Schottky diodes were prepared using a one side polished n-InP wafer with donor concentration of 4.9–5.0 $\times$ 10^{15} cm^{-3} (given by the manufacturer). The wafer was cleaned with warm organic solvents like trichloroethylene, acetone and methanol by means of ultrasonic agitation for the duration of 5 min each step to remove contaminants, followed by rinsing in deionized (DI) water and drying in N_2 flow. The wafer was then etched with HF (49%) and H_2O (1:10) to remove the native oxides from the substrate. Prior to deposition of organic layer on the n-InP substrate, the ohmic contacts were made by evaporating indium on the rough side of the n-InP. The contacts were then annealed at 350°C for 1 min in N_2 ambient. First, the PVA film was coated on smooth surface of n-type InP by spin-coating technique using spin coater (Delta spin-1) at a rotation speed of 2000 rpm for 5 min without any surface treatment. The thickness of the film so obtained was in the range of 10–20 nm across the whole substrate surface used is uniform. Finally, Au (50 nm) as a top metal electrode (diameter of 0.7 mm) was deposited by using e-beam evaporation system. The temperature-dependent I–V and C–V characteristics of the Au/PVA/n-InP Schottky structures were measured in the temperature range 175–425 K in steps of 25 K using a precision semiconductor parameter analyzer (Agilent-4155 C) and a precision LCR meter (Agilent-4248 A).

RESULTS AND DISCUSSION

Extraction of Schottky Diode Parameters from I–V and C–V Characteristics

Figure 1 shows the I–V characteristics of the as-deposited Au/PVA/n-InP Schottky diodes in the temperature range of 175–

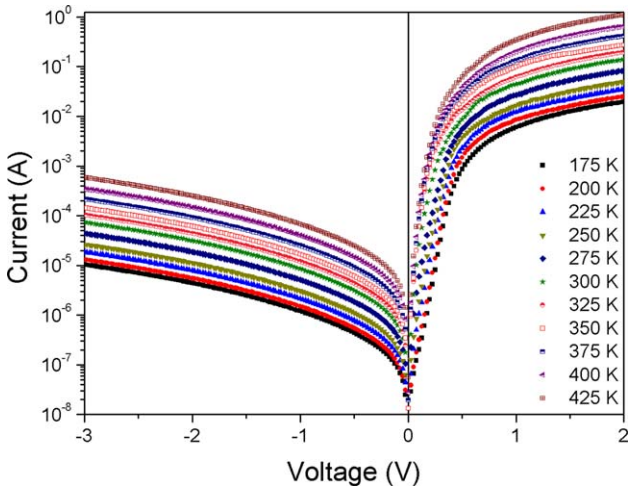

Figure 1. *I–V* characteristics of Au/PVA/n-InP Schottky structures measured at various temperatures. [Color figure can be viewed in the online issue, which is available at wileyonlinelibrary.com.]

425 K. It is found that the leakage currents at −1 V, is increases with an increase in temperature and the values are range from 1.20×10^{-6} A (at 175 K) to 6.81×10^{-5} A (at 425 K). To achieve the SBH and the ideality factor (n), the forward bias characteristics in terms of thermionic emission (TE) over the barrier can be analyzed as[3]

$$I = AT^2A_R^*\exp\left(-\frac{q\varphi_{bo}}{k_BT}\right)\exp\left(\frac{qV}{nk_BT}\right) = I_o\exp\left(\frac{qV}{nk_BT}\right), \quad (1)$$

The pre-factor I_o is the saturation current, T is the absolute temperature, k_B is the Boltzmann's constant, n is the ideality factor, φ_{bo} is the SBH, and A_R^* is the modified Richardson constant, is assumed to be 9.4 A/cm^2 K^2 for n-InP.[24] From eq. (1), the ideality factor n can be written as

$$n = \frac{q}{k_BT}\left(\frac{dV}{d\ln(I)}\right) \quad (2)$$

The experimental values of φ_{bo} and n are determined from intercepts and slopes of the forward bias ln I versus V plot at each temperature using TE theory, respectively. The values of the experimental φ_{bo} and n for the device is 0.23 eV and 4.39 (at 175 K) and 0.85 eV and 2.2 (at 425 K). Generally, Schottky barrier to n-InP yield low barrier contacts. The SBH values of 0.44, 0.46, 0.48, and 0.51 eV at 300 K obtained by Benamara et al.,[25] Szydlo et al.,[26] Ucar et al.,[27] and Shi et al.,[28] respectively. Further, Soylu et al.[19] found that the BH of Au/pyronine-B/moderately doped n-InP contact was 0.66 eV. In our work, it is found that the interfacial layer of PVA increases the BH (0.63 eV) at 300 K by the influence of the space charge region of the Au/n-InP Schottky junction. The increase or decrease in effective barrier height for the organic modified Schottky diode may be due to the energy level alignment of the lowest unoccupied molecular orbital (LUMO) with respect to the conduction band minimum (CBM) of the inorganic semiconductor at the organic/inorganic semiconductor interface. This interface difference in vacuum levels is attributed to interface dipoles. In fact, modification of semiconductor surfaces by molecules can lead to the changes in the electronic properties of the metal/semiconductor junctions.

The experimental reverse bias C^{-2}–V characteristics of the Au/PVA/n-InP Schottky diode over the temperature range of 175–425 K. The junction capacitance has been measured at a frequency of 1 MHz. In Schottky diodes, the depletion capacitance is expressed as[3]

$$C = \left[\left(\frac{q\varepsilon N_SA^2}{2}\right)\left(V_{bi} - \frac{k_BT}{q} - V_R\right)\right]^{\frac{1}{2}}, \quad (3)$$

where ε_S is the permittivity of the semiconductor ($\varepsilon_S = 11\ \varepsilon_o$) and N_d is the doping density. The x-intercept of the plot of ($1/C^2$) versus V_R is V_o and related to built-in potential V_{bi} by the equation $V_{bi} = V_o + k_BT/q$, where T is the absolute temperature. The BH is given by $\varphi_{bo}^{CV} = V_{bi} + V_n$, where $V_n = (k_BT/q)\ln(N_c/N_d)$. The density of states in the conduction band edge is given by $N_c = 2(2\pi m^* kT/h^2)^{3/2}$ (at room temperature $N_c = 5.7 \times 10^{17}$ cm^{-3} for InP). The values of N_c varied from 2.62×10^{17} cm^{-3} to 9.44×10^{17} cm^{-3} in the temperature range of 175–425 K, respectively. In addition, the temperature dependence of the experimental donor concentration (N_d) is determined from reverse bias C^{-2}–V characteristics. A plot of N_d values as a function of temperature is shown inset of Figure 2. The estimated values of N_d are varied from 2.24×10^{15} cm^{-3} to 4.79×10^{15} cm^{-3} for the n-type InP wafer in the temperature range between 175 and 425 K. As shown from inset of Figure 2, the donor concentration of the n-InP slightly decreases as temperature decreases. At low temperatures, mostly all impurities are frozen out and cause a strong increase in the R_S of the diode, which makes the measure capacitance to appear smaller. More electrons may be frozen at the donor level in the freeze-out region and conduction mechanisms in the freeze-out region are complex. As a donor concentration decreases then capacitance also decreases with decreasing temperature. The experimental values of φ_{bo}^{CV} are 0.89 eV at 175 K and 0.61 eV at 425 K.

Further, it is noted from Table I, the barrier heights (BH) increase in *I–V* technique and decrease in *C–V* technique which may be due to the biasing modes. According to thermionic

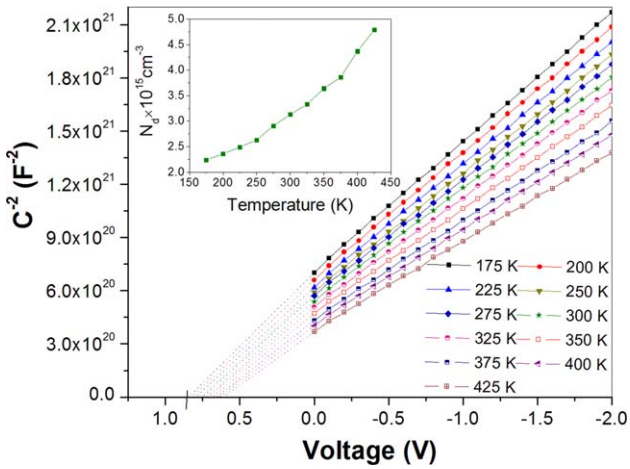

Figure 2. The experimental reverse bias C^{-2}–V plots of Au/PVA/n-InP Schottky structures for different temperatures at 1 MHz frequency. Variation of the donor concentrations from *C–V* characteristics at different temperatures is shown in the inset. [Color figure can be viewed in the online issue, which is available at wileyonlinelibrary.com.]

Table I. The Temperature Dependent Parameters of n, φ_{bo}, and N_d Determined from φ_{bo}^{IV} (eV) and φ_{bo}^{CV} (eV) Measurements in the Temperature Range of 175–425 K for Au/PVA/n-InP Schottky Structures

Temperature (K)	φ_{bo}^{IV} (eV)	Ideality factor (n)	φ_{bo}^{CV} (eV)	$N_d \times 10^{15}$ (cm^{-3})
175	0.23	4.39	0.89	2.24
200	0.33	3.91	0.88	2.36
225	0.41	3.56	0.86	2.49
250	0.47	3.25	0.84	2.63
275	0.53	2.99	0.82	2.91
300	0.63	2.78	0.80	3.13
325	0.70	2.63	0.77	3.33
350	0.75	2.49	0.74	3.64
375	0.79	2.36	0.70	3.86
400	0.82	2.27	0.65	4.37
425	0.85	2.20	0.61	4.79

theory (TE) mechanism, the zero-bias barrier height φ_{bo}^{IV}calculated from I–V characteristics is found to increase with increasing temperature where biasing mode is forward biased. The increase of $\varphi_{bo}^{IV}$with temperature is ascribed to homogeneity of the Schottky barrier at the metal/semiconductor junction. For an inhomogeneous barrier, the effective BH for TE increases with temperature due to the spreading of electric field distribution of charge carriers.[29] Though, the BH determined from the C^{-2}–V characteristics at high frequency decreased linearly with increasing temperature where biasing mode is reverse biased. The BH determined from C–V technique, φ_{bo}^{CV} is governed by depletion region thickness and this is less sensitive to small scale inhomogeneity.[30]

Furthermore, the discrepancy between $\varphi_{bo}^{CV}$and φ_{bo}^{IV} can be explained by the existence of excess capacitance and SBH inhomogeneities.[31–33] The reason for this discrepancy between the measured SBHs is clear. The current in the I–V measurement is dominated by the current which flows through the region of low SBH, and the measured I–V SBH is significantly lower than the weighed arithmetic average of the SBHs. Conversely, the barrier height measured from the C–V or flat band is influenced by the distribution of charge at the depletion region boundary and this charge distribution follows the weighted arithmetic average of the SBHs. As a result, the SBH calculated from the zero-bias intercept assuming TE as a current transport mechanism is well below the C–V or flat-band measured BH and the weighted arithmetic average of SBHs.

Effect of Thermionic Field Emission

The high values of ideality factor and its temperature dependence suggest that the current transport is predominated by thermionic field emission (TFE).[34] If the current transport is controlled by the TFE theory, the I–V characteristics of Au/PVA/n-InP Schottky structure can be given by[35]

$$I = I_o \exp\left(\frac{qV}{E_0}\right) \tag{4}$$

with

$$E_0 = E_{00}\coth\left(\frac{E_{00}}{k_BT}\right) = n_{tun}k_BT = \frac{qE_{00}}{k_BT}\coth\left(\frac{qE_{00}}{k_BT}\right) \tag{5}$$

The characteristic tunneling energy (E_{00}) parameter is related to the tunneling transmission probability and is given by[36]

$$E_{00} = \frac{h}{4\pi}\sqrt{\left(\frac{N_d}{m^*\varepsilon_s}\right)} \tag{6}$$

The calculated values of E_{00} are 1.31 meV at 425 K and 0.88 meV at 175 K, respectively. To find, the dominant current transport mechanism of the Au/PVA/n-InP Schottky structure, we normalized E_{00} with k_BT in the investigated temperature range. Figure 3 reveals, E_{00}/k_BT values increase with decreasing in temperatures and temperature and E_{00}/k_BT « 1 is satisfied for the investigated temperature range. According to the theory, field emission (FE) becomes important when E_{00}/k_BT » 1 whereas, TFE dominates when $E_{00}/k_BT \approx 1$ and TE is dominates if E_{00}/k_BT « 1. Therefore, we can suggest that all over the temperature range TE is the predominant current conduction mechanism. From eq. (5), the ideality factor of Au/PVA/n-InP according to TFE results as 1.08 at 175 K and 1.19 at 425 K, respectively. These values are too low when comparing to our measured values (from I–V characteristics) and are constancy over the entire temperature range. The calculated values are very close to unity for the wide temperature range (175–425 K). Consequently, the tunneling current is not useful for calculation of BH and ideality factors. Then, the origin of the TFE and FE can be ruled out. Therefore, the higher ideality factor values may be related to TE over a Gaussian barrier height distribution.

Density of Interface States

To increase the quality of devices fabricated using the inorganic with organic like as organic/inorganic structures. These structures can be useful for decreasing surface states, surface damage and contamination. In fact, communication of the interface states with metal by tunneling decrease with increasing interfacial layer thickness. Accordingly, if there is a sufficient thick oxide layer between the metal and the semiconductor, the

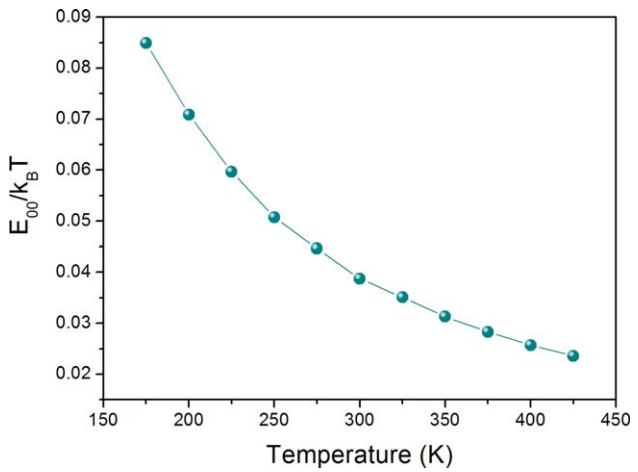

Figure 3. The plot of normalized E_{00}/k_BT values as a function of temperature. [Color figure can be viewed in the online issue, which is available at wileyonlinelibrary.com.]

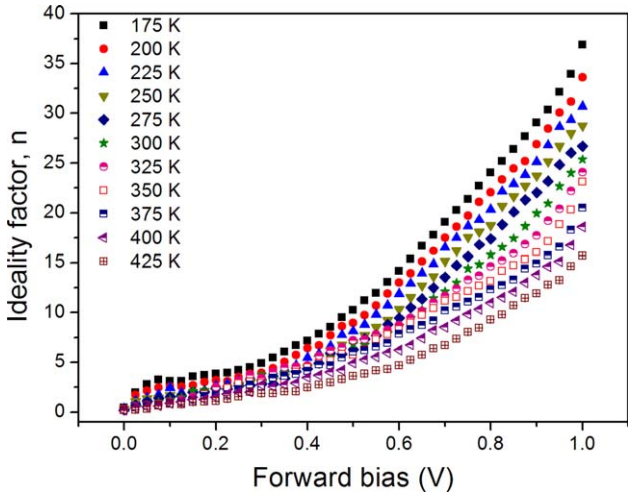

Figure 4. Plots of the forward bias dependent ideality factor $n(V,T)$ for Au/PVA/n-InP Schottky structure at different temperatures. [Color figure can be viewed in the online issue, which is available at wileyonlinelibrary.com.]

change in occupancy of the interface states in equilibrium with the semiconductor is determined by the change in energy of the state relative to the Fermi energy in the semiconductor.[37]

The bias dependence of the SBH is described in terms of the dependence of the ideality factor on the applied bias due to surface states, and shift in BH with forward bias V is given by[1,38,39]

$$\varphi_e(V)-\varphi_{0Bn}=\left(1-\frac{1}{n(V)}\right)(V-IR_S) \tag{7}$$

From eq. (1), the ideality factor directly determined for each measuring temperature at any given forward bias from the slope of the $\ln I-V$ characteristics: $n(V)=(q/k_BT)(dV/d\ln I)$. Figure 4 shows the plots of the forward bias-dependent ideality factor $n(V)$ at various temperatures taken from the experimental temperature dependent $\ln I-V$ measurements of Au/PVA/n-InP Schottky structure given in Figure 1. It is clearly observed from Figure 1, the ideality factor is varying slowly respective to forward bias in the region where the influence of the series resistance (R_SI) is small and followed by a large varying function of the forward bias where the influence of the series resistance is dominates the $\ln I-V$ measurements. Then, the latter influence gives rise to the curvature at higher current in the semilogarithmic I–V plot. Moreover, divided thee parts of semilog I–V plot as: the low-forward bias region where the recombination current can dominate the current flow, the linear region where the TE assumption can be applicable and the upper current range where the influence of the series resistance is high. Our Au/PVA/n-InP Schottky structures clearly shows ideality factor larger than unity in the linear region. The downward curvature of forward bias semilog I–V plots shows a deviation in ideality factor at high current is due to the interfacial layer thickness, the interface state density and series resistance. That is, it can be concluded that the BH and other characteristic parameters are mostly controlled by the interface states and play an important role between conducting polymer/semiconductor interface. The density distribution of interface states (N_{SS}) in equilibrium with the semiconductor can be determined from the forward bias I–V data by taking the voltage-dependent ideality factor $n(V,T)$ with effective barrier height $(\varphi_b(V,T))$. The parameters of $n(V,T)$ and $\varphi_b(V,T)$ can be determined from the following equations.[40]

$$n(V)=\frac{q}{k_BT}\left[\frac{V}{\ln(I/I_o)}\right]=1+\frac{\delta}{\varepsilon}\left[\frac{\varepsilon_S}{W_D}+qN_{SS}\right] \tag{8}$$

$$\varphi_b(V,T)=\varphi_{bo}^{IV}+\beta V=\varphi_{bo}^{IV}+\left(1-\frac{1}{n(V,T)}\right) \tag{9}$$

where W_D is the space charge region width, δ is the thickness of interfacial organic layer, ε_i and ε_S are the permittivities of the interfacial layer and semiconductor, and $\beta\left(=d\varphi_{\text{eff}}/dV=1-1/n(V)\right)$ is the change in effective BH with bias voltage. For Au/PVA/n-InP Schottky structure having interface states in equilibrium with the semiconductor, the ideality factor becomes greater than unity as proposed by Card and Rhoderick,[40] and interface state density (N_{SS}) is given by

$$N_{SS}(V)=\frac{1}{q}\left[\frac{\varepsilon_i}{\delta}\left(n(V,T)-1\right)-\frac{\varepsilon_S}{W}\right] \tag{10}$$

Furthermore, in n-type semiconductors, the energy interface states with respect to the conduction band edge (E_C–E_{SS}) are obtained as

$$E_C-E_{SS}=q(\varphi_e-V) \tag{11}$$

Substituting in eq. (8) the values of the voltage dependence of n(V), δ, and W_D, the values of N_{SS} as a function of (E_C–E_{SS}) are obtained which are shown in Figure 5. The N_{SS} value of Au/PVA/n-InP Schottky structures decreases with increasing E_C–E_{SS} values as a function of temperature. Moreover, the exponential growth of the N_{SS} toward the top of the valance band is very noticeable. Such behavior of N_{SS} is a result of molecular restructuring and reordering of PVA and InP molecules at the metal/semiconductor interface under the influence of temperature.[41] From Figure 5, a typical results of the interface state density (N_{SS}) range from E_C–0.21 eV to E_C–0.29 eV at 175 K and E_C–0.49 eV to E_C–0.70 eV at 425 K. The magnitude of the interface

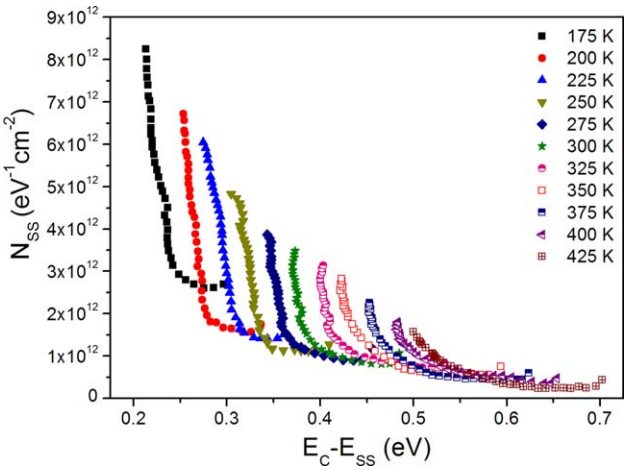

Figure 5. Interface state density N_{SS} as a function of E_C–E_{SS} for the Au/PVA/n-InP Schottky structure at different temperatures. [Color figure can be viewed in the online issue, which is available at wileyonlinelibrary.com.]

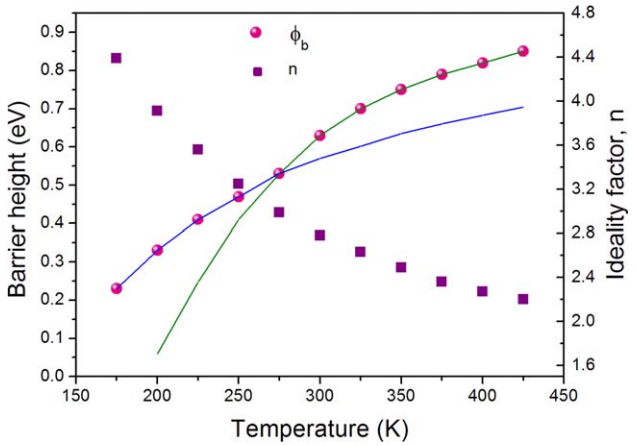

Figure 6. Zero-bias SBH an ideality factor as a function of temperature for Au/PVA/n-InP Schottky structure the dotted and solid lines without symbols are for the calculated SBHs using (14) for double Gaussian distributions of BHs in temperature range (175–275 K: Distribution 1) and (300–425 K: Distribution 2), respectively. [Color figure can be viewed in the online issue, which is available at wileyonlinelibrary.com.]

state density (N_{SS}) at 175 K is varied from 2.69 × 10^{12} $eV^{-1}cm^{-2}$ (E_C–0.29 eV) to 8.24 × 10^{12} eV^{-1} cm^{-2} (E_C–0.21 eV) and the magnitude of the interface state density (N_{SS}) at 425 K is varied from 4.32 × 10^{11} eV^{-1} cm^{-2} (E_C–0.70 eV) to 1.56 × 10^{12} eV^{-1} cm^{-2} (E_C–0.49 eV). These values are similar to the results reported in the literature.[42,43] It is well known that the interface traps charges, which are the charges located the insulator/semiconductor interface with energy states in the semiconductor forbidden band gap. When the thickness of insulator layer is >30 Å, interface trapped charges are entirely depend by the semiconductor.[44] As a result, the forward bias *I–V* characteristics deviate from the ideal case where as the ideality factor is controlled by the interface states. These surface states nonuniformly distributed in the semiconductor band gap are directly proportional to the temperature.

Barrier Inhomogeneities

The experimental values of zero-bias BH dependence are irrespective of temperature, whereas the *n* decreases with increasing temperature. This indicates that the current transport deviates from the ideal TE model. Because the current transport across the Schottky structure interface is a temperature-activated process, electrons at low temperatures are able to surmount the lower barriers.[4,45] The temperature dependence of zero-bias BH and ideality factor is shown in Figure 6. At the over temperature 300 K observed that the variations of the SBH and ideality factor with temperature are limited. Under temperature 300 K, a respective increase and decrease of ideality factor and BH is observed with decreasing temperature. Similar results have already been reported in literature for other semiconductor contacts. For instance, Tung et al. showed that the presence of a wide distribution of low SBH patches caused by a laterally inhomogeneous barrier could be attributed to a higher ideality factor. Moreover, an ideality factor value greater than the unity could be due to the mechanisms such as the image force effect, recombination-generation, and tunneling.[46] Therefore, the current transport will be dominated by the current flowing through the patches of lower SBH, leading to a larger ideality factor, attributed to secondary mechanisms at the interface such as lateral inhomogeneous distribution of BH which may be created by interface defects.

Interestingly, it is noted that the experimental value of ideality factor is found to be decreased with an increase in temperature. It is observed from Figure 7, at higher temperatures, n is nearly equal to unity and shows temperature dependent, which may be described as the "T_0 effect or anomaly." Such behavior of the ideality factor has been attributed to the inhomogeneities in the Schottky barrier.[1] When the temperature is lowered, the function current is dominated by low-SBH regions with lower-effective SBH and larger ideality factors.[45–47] In addition, the ideality factors are not constant with temperature, and they shows linear behavior with inverse temperature. The ideality factor of the diodes showing this behavior varies with temperature as

$$n(T) = n_0 + \frac{T_0}{T} \tag{12}$$

where, the n_0 and T_0 are constants which are found to be 0.61 and 660 K, respectively. The increase in the ideality factor with decreasing temperature is known as the T_0 effect. Explanations of the possible origin of such case have been proposed taking into account the interface state density distribution, quantum mechanical tunneling, and image force lowering.[3] In fact, the forward bias *I–V* characteristics of the Au/PVA/n-InP Schottky structure explained on the basis of the TE theory reveal an abnormal decrease in the BH and a increase in the ideality factor with decreasing temperature, which leads to nonlinearity in the conventional activation energy plot of $\ln(I_o/T^2)$ versus $10^3/T$. Such nonlinear behavior of Au/PVA/n-InP Schottky structure at low temperature in the forward bias can be attributed to the special variation in the BHs. Similar observations like the behavior of BH and the ideality factor with the increasing temperature reported by several researchers.[45,47–49]

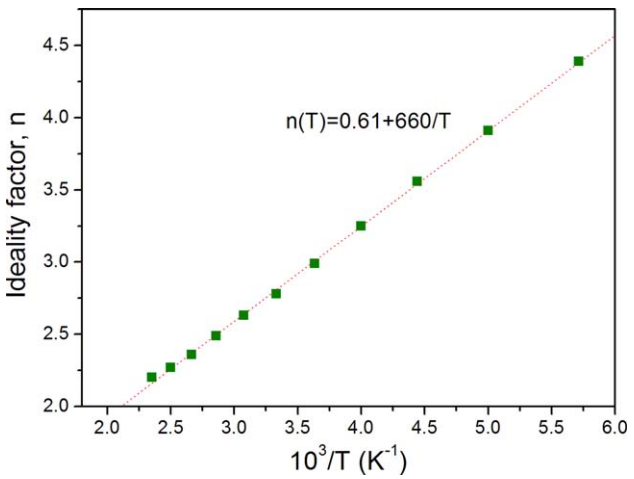

Figure 7. Temperature dependent of the ideality factor for the Au/PVA/n-InP Schottky structure. [Color figure can be viewed in the online issue, which is available at wileyonlinelibrary.com.]

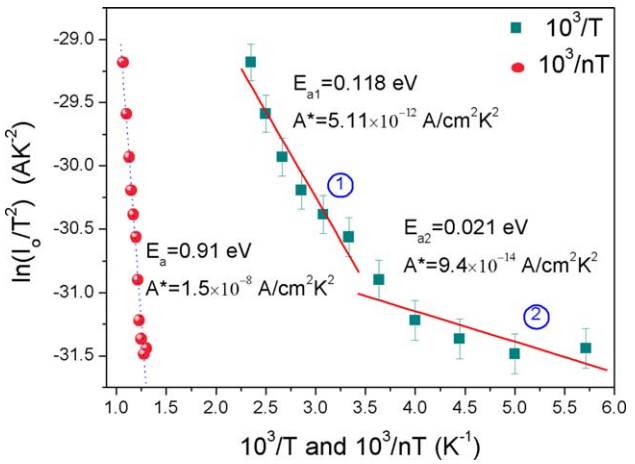

Figure 8. Conventional Richardson plots of the $\ln(I_o/T^2)$ versus $10^3/T$ and $10^3/nT$ for the Au/PVA/n-InP structure. [Color figure can be viewed in the online issue, which is available at wileyonlinelibrary.com.]

To extract the BH, one normally uses a conventional TE theory. However, there have been several reports about deviation from this classical TE theory.[49–53] To determine the BH in another way, the Richardson plot is drawn. Equation (2) can be rewritten as

$$\ln\left(\frac{I_o}{T^2}\right)=\ln\left(AA_R^*\right)-\frac{q\varphi_{bo}}{k_BT} \tag{13}$$

Figure 8 shows the conventional Richardson plot of $\ln(I_o/T^2)$ versus $10^3/T$ and $10^3/nT$. The temperature dependence of experimental $\ln(I_o/T^2)$ versus $10^3/nT$ gives a straight line. The values of the activation energy and Richardson constant were obtained from the slope of this straight line as 0.91 eV and 1.5 $\times$ 10^{-8} A/cm^2 K^2, respectively. However, the temperature dependent $\ln(I_o/T^2)$ versus $10^3/T$ plot has two linear temperature ranges. In the first region between 300 and 425 K (Distribution 1), the values of the activation energy and Richardson constant are obtained from the slope and intercept of this straight line as 0.118 eV and 5.11 $\times$ 10^{-12} A/cm^2 K^2, respectively, whereas in the second region between 175 and 275 K (Distribution 2), the values of the activation energy and Richardson constant are obtained from the slope and intercept of this straight line as 0.021 eV and 9.4 $\times$ 10^{-14} A/cm^2 K^2, respectively. These experimental Richardson constant values are much lower than the theoretical values of 9.4 A/cm^2 K^2 for n-InP. Above results elucidate that the deviation in Richardson plot may be due to the spatial inhomogeneous BH and potential fluctuation at the interface that consist of low and high barrier areas.[45,54–58] In addition, the current through the barrier will flow preferentially through the lower barriers in the potential distribution.

There is a linear correlation between the experimental zero-bias BH and ideality factors explained by Tung. A plot of the experimental zero-bias BH and ideality factor as a function of temperature is shown in Figure 9. There are two linear regions between the experimental zero-bias BHs and ideality factors of the Au/PVA/n-InP structure, which can be lateral inhomogeneities of BHs.[45,59] In the low temperature region (175–275 K, Distribution 2), the extrapolation of the experimental BH versus ideality factor plot to $n = 1$ gives a homogeneous barrier height of 0.98 eV. In the high temperature region (300–425 K, Distribution 1), the extrapolation of the experimental BH versus ideality factor plot to $n = 1$ gives the value of 0.80 eV. These results confirm that the current transport is not only due to TE in our diodes. Thus, is notify that the presence of double GDs, namely, GD1 and GD2 BHs in the contact area.

A GD of the BH (an analytical potential fluctuation model) introduced by Song et al.[60] can be used to explain the nonideal behavior of Au/PVA/n-InP Schottky structures, the *I–V* can still be well described by eq. (1), except that $\varphi_{bo}$and n should be replaced by $\varphi_{ap}$and n_{ap}. The GD of the BHs with a mean value $\bar{\varphi}_{bo}$and a standard deviation σ_o yields the following expression for the BH

$$\varphi_{ap}=\bar{\varphi}_{bo}(T=0)-\frac{q\sigma_o^2}{2k_BT} \tag{14}$$

where φ_{ap} is the apparent BH measured experimentally and the temperature dependence of σ_o is usually small and can be neglected.[45] The observed variation of ideality factor with temperature in the metal is given by[61]

$$\left(\frac{1}{n_{ap}}-1\right)=-\rho_2+\frac{q\rho_3}{2k_BT} \tag{15}$$

where n_{ap} is apparent ideality factor, ρ_2 and ρ_3 are the voltage coefficients, which may depend on temperature, and they quantify the voltage deformation of the BH distribution. The experimental φ_{ap} versus $q/2k_BT$ plots in Figure 10 are drawn to obtain evidence of a GD of the BHs. The calculated φ_{ap} versus $q/2k_BT$ and $(1/n_{ap}-1)$ versus $q/2k_BT$ plots (Figure 10) drawn by means of the data obtained from Figure 1 respond to two lines instead of a single straight line with transition occurring at 300 K. These observations indicate of two GD BHs in the contact area. The intercept and slope of this straight lines gives two set of values $\bar{\varphi}_{bo}$ of 1.246 eV and σ_o of 0.176 V in the temperature range of 300–425 K (Distribution 1) and 0.899 eV and

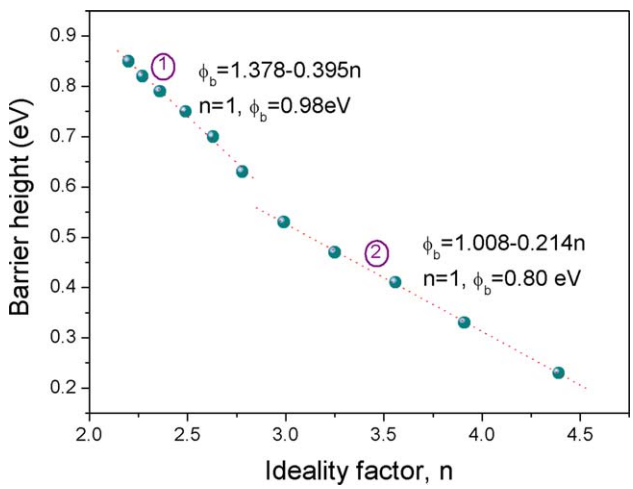

Figure 9. SBH versus ideality factor of the Au/PVA/n-InP Schottky structure at various temperatures. [Color figure can be viewed in the online issue, which is available at wileyonlinelibrary.com.]

0.137 V in the temperature range of 175–275 K (Distribution 2). Similar results showed by Chand and Kumar,[49] the existence of a double GD in the metal/semiconductor contacts can be attributed to the nature of the inhomogeneities themselves in the two cases. This may involve variation in the interface composition/phase, interface quality, electrical charges and nonstoichiometry, etc. Further, such inhomogeneities might occur on a scale that inhibits their detection by the usual characterization tools. They influence the *I–V* characteristics of the Schottky diodes at particularly low temperatures. Hence, *I–V* measurements at very low temperatures are capable of revealing the nature of barrier inhomogeneities present in the contact area. Furthermore, these results have shown that the temperature dependence characteristics of Au/PVA/n-InP Schottky structures can be explained on the basis of a TE mechanism with double GD of the BHs.

Likewise, the plot of $(1/n_{ap}-1)$versus $q/2k_BT$(Figure 10) should also possess different characteristics in the two temperature ranges because the Au/PVA/n-InP diode contains two BH distributions. The values of $\rho_2$obtained from the intercepts of the experimental $(1/n_{ap}-1)$versus $q/2k_BT$plot are 0.488 V in the 300–425 K range (Distribution 1) and 0.313 V in the 175–275 K range (Distribution 2), whereas the values of $\rho_3$from the slopes are 0.017 V in 300–425 K range (Distribution 1) and 0.009 V in the 175–275 K range (Distribution 2). The linear behavior of this plot reveals that the ideality factor does indeed express the voltage deformation of the GD of the BH. According to these results, this inhomogeneities and potential fluctuation in the barrier dramatically affect low temperature *I–V* characteristics. As shown from the experimental $(1/n_{ap}-1)$versus $q/2k_BT$plot, ρ_3 value or the slope of Distribution 1 is larger than Distribution 2. Therefore, we can say that the Distribution 2 at very low temperatures may possibly take place due to some phase change on cooling below a certain temperatures. A similar behavior of double GD has been observed by Huang et al.[62] and Gullu et al.[63]

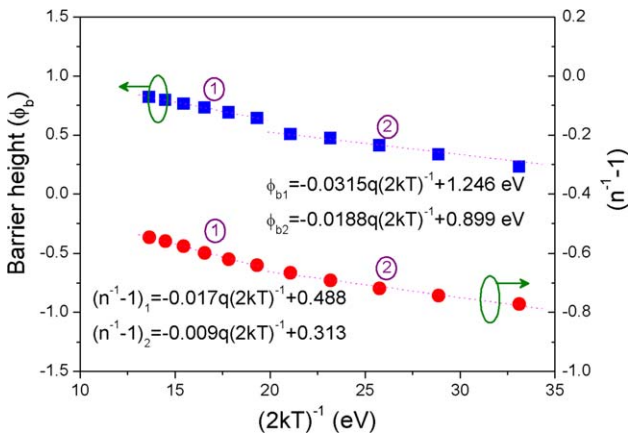

Figure 10. φ_{ap} versus $q/2k_BT$ and $(n_{ap}^{-1}-1)$ versus $q/2k_BT$ curves of an Au/PVA/n-InP Schottky structure according to the double GD of BHs. The data show linear variation in the two temperature ranges with a transition around 275 K. [Color figure can be viewed in the online issue, which is available at wileyonlinelibrary.com.]

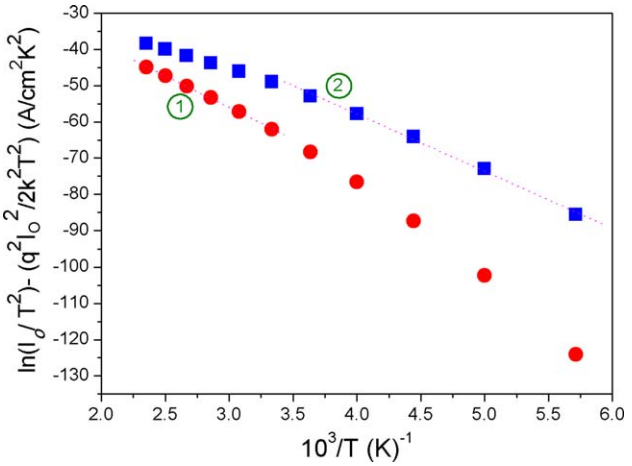

Figure 11. Modified Richardson $\ln(I_o/T^2)-(q^2\sigma_o^2/2k_B^2T^2)$ versus $10^3/T$ plot of the Au/PVA/n-InP Schottky structure according to the double GD of BHs. [Color figure can be viewed in the online issue, which is available at wileyonlinelibrary.com.]

Moreover, as indicated earlier, the conventional activation energy $\ln(I_o/T^2)$versus $10^3/T$ plot has showed nonlinearity at low temperatures. To explain these behaviors, a combination of eqs. (1) and (14) can be written as

$$\ln\left(\frac{I_o}{T^2}\right)-\left(\frac{q^2\sigma_o^2}{2k_B^2T^2}\right)=\ln\left(AA_R^*\right)-\frac{q\bar{\varphi}_{bo}}{k_BT} \tag{16}$$

Figure 11 shows modified conventional activation energy $\ln(I_o/T^2)-(q^2\sigma_o^2/2k_B^2T^2)$versus $10^3/T$plot. Two straight lines (Figure 11) with transition occurring at 300 K, and according to eq. (10), the slope of these straight lines directly yields the mean BHs ($\bar{\varphi}_{bo}$) and intercept ($=\ln A_R^*$) at the ordinate determines $A_R^*$for a given Schottky contact area. Thus, the $\ln(I_o/T^2)-(q^2\sigma_o^2/2k_B^2T^2)$values were calculated for both two values of σ_o obtained in the temperature ranges of (175–275 K) and (300–425 K). As shown in Figure 11, the closed circles and closed squares, it gives BH values 0.71 eV in 175–275 K range (Distribution 2) and 1.17 eV in 300–425 K range (Distribution 1). The intercept at the ordinate gives the Richardson constant A_R^* as 6.9 A/cm^2 K^2 in 175–275 K range (Distribution 2) and 9.9 A/cm^2 K^2 in 300–425 K range (Distribution 1) without the temperature coefficient of the BHs. The obtained Richardson constant values (9.9 A/cm^2 K^2) are close to the theoretical values of 9.4 A/cm^2 K^2 for n-type InP.

CONCLUSIONS

The influence of a thin polyvinyl alcohol (PVA) interlayer on the electrical characteristics of Au/n-InP Schottky contacts have been investigated in the wide temperature range of 175–425 K by using *I–V* and *C–V* measurements. The interface states density is extracted from both the forward bias dependence of the SBH and ideality factor. Experimental results reveal an abnormal decrease in the zero-bias barrier height (φ_{bo}^{TE}) and increase in the ideality factor (n) with decreasing temperature. Electrical properties also confirm that the temperature dependent *I–V* characteristics of Au/PVA/n-InP Schottky structure can be successfully explained on the basis of double GD of the BHs. The

double GD has mean BHs ($\bar{\varphi}_{bo}$) of 1.246 and 0.899 eV and standard deviation (σ_o) of 0.176 and 0.137 V, respectively. Thus, the values of $\bar{\varphi}_{bo}$and Richardson constants (A_R^*) are obtained from a modified conventional energy $\ln(I_o/T^2)-(q^2\sigma_o^2/2k_B^2T^2)$versus $10^3/T$ plot as two temperature regions as 0.71 eV and 6.9 A/cm^2 K^2 (175–275 K), 1.17 eV and 9.9 A/cm^2 K^2 (300–425 K), respectively. This value of the effective Richardson constant, 9.9 A/cm^2 K^2, is very close to the theoretical value of 9.4 A/cm^2 K^2 for n-InP. Furthermore, we have reported that the experimental data of the Au/PVA/n-InP Schottky structure can be explained by assuming the existence of double GD distributions in the wide temperature range.

ACKNOWLEDGMENTS

This work was supported by Kyungpook National University Research Fund 2012, 2008 Brain Korea 21 (BK21), the National Research Foundation of Korea grants funded by MEST (2012-0005671, 2012-0000627), R&D program of MKE/KETEP (2011101050017B), WCU (World Class University) program (grant R33-10055), IT R&D program of MKE/KEIT (10038766), and the IT R&D program of MKE/KEIT (10038766) and MOTIE through the industrial infrastructure program (grant 10033630).

REFERENCES

1. Rhoderick, E. H.; Williams, R. H. Metal-Semiconductor Contacts; Clarendon Press: Oxford, **1978**.
2. Cowley, A. M.; Sze, S. M. *J. Appl. Phys.* **1965**, *36*, 3212.
3. Sze, S. M. Physics of Semiconductors; Wiley: New York, **1981**.
4. Werner, J. H.; Guttler, H. H. *J. Appl. Phys.* **1991**, *69*, 1522.
5. Gull, O.; Aydogan, S.; Turut, A. *Microelectron. Eng.* **2008**, *85*, 1647.
6. Abay, B.; Onganer, Y.; Saglam, M.; Efeoglu, H.; Turut, A.; Yogurtcu, Y. K. *Microelectron. Eng.* **2000**, *51–52*, 689.
7. Gupta, R. K.; Singh, R. A. *Mater. Chem. Phys.* **2004**, *86*, 279.
8. Gupta, R. K.; Singh, R. A. *Mater. Sci. Semicond. Process* **2004**, *7*, 83.
9. Huang, L.-M.; Wen, T.-C.; Gopalan, A. *Thin Solid Films* **2005**, *473*, 300.
10. Nguyen, V. C.; Potje-Kamloth, K. *Thin Solid Films* **1999**, *142*, 338.
11. Zhang, J.; Jiang, F. *Chem. Phys.* **2003**, *289*, 243.
12. Dharmaraj, N.; Kim, C. H.; Kim, H. Y. *Synth. React. Inorg. Met-Org. Chem.* **2006**, *36*, 29.
13. Bazuev, G. V.; Gyrdasova, O. I.; Grigorov, I. G.; Koryakova O. V. *Inorg. Mater.* **2005**, *41*, 288.
14. Uslu, I.; Baser, B.; Yayh, A.; Aksu, M. L. *e-Polymers* **2007**, *145*, 1.
15. Saito, H.; Stuhn, B. *Polymer* **1994**, *35*, 475.
16. Ashok Kumar, A.; Rajagopal Reddy, V.; Janardhanam, V.; Seo, M.-W.; Hong, H.; Shin, K.-S.; Choi, C.-J. *J. Electrochem. Soc.* **2012**, *159*, H33.
17. Rajagopal Reddy, V.; Siva Pratap Reddy, M.; Ashok Kumar, A.; Choi, C.-J. *Thin Solid Films* **2012**, *520*, 5715.
18. Gullu, O.; Cankaya, M.; Baris, O.; Turut, A. *Microelectron. Eng.* **2008**, *85*, 2250.
19. Soylu, M.; Abay, B.; Onganer, Y. *J. Alloy Compd.* **2011**, *509*, 5105.
20. Dokme, I.; Altindal, S.; Tunc, T.; Uslu, I. *Microelectron. Reliab.* **2010**, *50*, 39.
21. Tunc, T.; Altindal, S.; Uslu, I.; Dokme, I.; Uslu, H. *Mater. Sci. Semicond. Process* **2011**, *14*, 139.
22. Demirezen, S.; Altindal, S.; Uslu, I. *Curr. Appl. Phys.* **2013**, *13*, 53.
23. Ozavci, E.; Demirezen, S.; Aydemir, U.; Altindal, S. *Sens. Actuators A* **2013**, *194*, 259.
24. Williams, R. H.; Robinson, G. Y.; Wilmsen C. W. Physics and Chemistry of III-V Compound Semiconductor Interfaces; Plenum Press: New York, **1985**.
25. Benamara, Z.; Akkal, B.; Talbi, A.; Gruzza, B.; Bideux, L. *Mater. Sci. Eng. C* **2002**, *21*, 287.
26. Szydlo, N.; Olivier, J. *J. Appl. Phys.* **1979**, *50*, 1445.
27. Ucar, N.; Ozdemir, A. F.; Aldemir, D. A.; Cakmak, S.; Calik, A.; Yildiz, H.; Cimilli, F. *Superlattices Microstruct.* **2010**, *47*, 586.
28. Shi, Z. Q.; Wallace, R. L.; Anderson, W. A. *Appl. Phys. Lett.* **1991**, *59*, 446.
29. Osvald, J.; Horvath, Zs. *Appl. Surf. Sci.* **2004**, *234*, 349.
30. Bozhkov, V. G.; Torkhov, N. A.; Shmargunov, A. V. *J. Appl. Phys.* **2011**, *109*, 073714.
31. Yakuphanoglu, F.; Senkel, B. F. *J. Phys. Chem. C* **2007**, *111*, 1840.
32. Chattopadhyay, S.; Bera, L. K.; Maiti, C. K.; Ray, S. K.; Bose, P. K.; Dentel, D.; Kubler, L.; Bischoff, J. L. *J. Mater. Sci. Mater. Electron.* **1998**, *9*, 403.
33. Altindal, S.; Karadeniz, S.; Tugluoglu, N.; Tataroglu, A. *Solid State Electron.* **2003**, *47*, 1847.
34. Kim, H.; Ryou, J.; Dupuis, R. D.; Lee, S. N.; Park, Y.; Jeon, J.W.; Seong, T.-Y. *Appl. Phys. Lett.* **2008**, *93*, 192106.
35. Tung, R. T. *Mater. Sci. Eng. R* **2001**, *35*, 1.
36. Cinar, K.; Yildirim, N.; Coskun, C.; Turut, A. *J. Appl. Phys.* **2009**, *106*, 073717.
37. Altindal, S.; Dokme, I.; Bulbul, M. M.; Yalcin, N.; Serin, T. *Micrelectron. Eng.* **2006**, *83*, 499.
38. Turut, A.; Saglam, M.; Efeoglu, H.; Yalcin, N.; Yildirim, M.; Abay, B. *Physica B* **1995**, *205*, 41.
39. Mamor, M. *J. Phys.: Condens. Matter.* **2009**, *21*, 335802.
40. Card, H. C.; Rhoderick, E. H. *J. Phys. D Appl. Phys.* **1971**, *4*, 1589.
41. Akkal, B.; Benamara, Z.; Boudissa, A.; Bouiadjra, N. B.; Amrani, M.; Bideux, I.; Gruzza, B. *Mater. Sci. Eng. B* **1998**, *55*, 162.
42. Pakma, O.; Serin, N.; Serin, T.; Altindal, S. *Semicond. Sci. Technol.* **2008**, *23*, 104014.
43. Pur F. Z.; Tataroglu, A. *Phys. Scr.* **2012**, *86*, 035802.

44. Sze, S. M.; Kwog, K. Ng. Physics of Semiconductor Devices; Wiley: New Jersey, **2007**.
45. Karatas, S.; Altindal, S.; Turut, A.; Ozmen, A. *Appl. Surf. Sci.* **2003**, *217*, 250.
46. Tung, R. T. *Phys. Rev. B* **1992**, *45*, 13509.
47. Sullivan, J. P.; Tung, R. T.; Pinto, M. R.; Graham, W. R. *J. Appl. Phys.* **1991**, *70*, 7403.
48. Zeyrek, S.; Altindal, S.; Yuzer, H.; Bulbul, M. M. *Appl. Surf. Sci.* **2006**,*252*, 2999.
49. Chand, S.; Kumar, J. *Semicond. Sci. Technol.* **1996**, *11*, 1203.
50. Chand, S.; Kumar, J. *Appl. Phys. A* **1997**, *65*, 497.
51. Horvath, Zs. J.; Dozsa, L.; Krafcsik, O. H.; Mohacsy, T.; Vida, Gy. *Appl. Surf. Sci.* **2004**, *234*, 67.
52. Altindal, S.; Kanbur, H.; Yildiz, D. E.; Parlak, M. *Appl. Surf. Sci.* **2007**, *253*, 5056.
53. Cvikl, B.; Korosak, D.; Horvath, Zs. J. *Vacuum* **1998**, *50*, 385.
54. Duman, S.; Gurbulak, B.; Turut, A. *Appl. Surf. Sci.* **2007**, *253*, 3899.
55. Dobrocka, E.; Osvald, J. *Appl. Phys. Lett.* **1994**, *65*, 575.
56. Jones, F. E.; Wood, B. P.; Myers, J. A.; Daniels, C. H.; Lonergan, M. C. *J. Appl. Phys.* **1999**, *86*, 6431.
57. Lonergan, M. C.; Jones, F. E. *J. Chem. Phys.* **2001**, *115*, 433.
58. Wenckstern, H. V.; Biehne, G.; Rahman, R. A.; Hockmuth, H.; Lorenz, M.; Grundmann, M. *Appl. Phys. Lett.* **2006**, *88*, 092102.
59. Schmitsdorf, R. F.; Kampen, T. U.; Monch, W. *Surf. Sci.* **1995**, *324*, 249.
60. Song, Y. P.; van Meirhaeghe, R. L.; Laflere, W. H.; Cardon, F. *Solid-State Electron.* **1986**, *29*, 633.
61. Chand, S.; Kumar, J. *Semicond. Sci. Technol.* **1995**, *10*, 1680.
62. Huang, S.; Lu, F. *Appl. Surf. Sci.* **2006**, *252*, 4027.
63. Gullu, O.; Biber, M.; Duman, S.; Turut, A. *Appl. Surf. Sci.* **2007**, *253*, 7246.